

# High pressures make Hg a transition metal in a thermodynamically stable solid

Xiaoli Wang<sup>1,2</sup>, Haiqing Lin<sup>1,3</sup>, Yanming Ma<sup>4,1</sup>, and Mao-sheng Miao<sup>5,1\*</sup>

<sup>1</sup>Beijing Computational Science Research Center, Beijing 10084, P. R. China

<sup>2</sup>Institute of Condensed Matter Physics, Linyi University, Linyi 276005, P. R. China

<sup>3</sup>Department of Physics and Institute of Theoretical Physics,  
Chinese University of Hong Kong, Hong Kong SAR, P.R. China

<sup>4</sup>State Key Lab of Superhard Materials, Jilin University, Changchun 130012, P.R. China and

<sup>5</sup>Materials Department and Materials Research Laboratory,  
University of California, Santa Barbara, CA 93106-5050

The appropriateness of including Hg among the transition metals has been debated for a long time. Although the synthesis of HgF<sub>4</sub> molecules in gas phase was reported before, the molecules show strong instabilities and dissociate. Therefore, the transition metal propensity of Hg remains an open question. Here, we propose that high pressure provides a controllable method for preparing unusual oxidation states of matter. Using an advanced structure search method based on first-principles electronic structure calculations, we predict that under high pressures, Hg can transfer the electrons in its outmost *d* shell to F atoms, thereby acting as a transition metal. Oxidation of Hg to the +4 state yielded thermodynamically stable molecular crystals consisting of HgF<sub>4</sub> planar molecules, a typical geometry for *d*<sup>8</sup> metal centers.

PACS numbers: 62.50.-p, 61.50.Ah, 61.50.Ks, 82.33.Pt, 81.40.Vw, 71.70.Fk

A goal of physics and chemistry is to prepare unusual states of matter beyond the naturally occurring forms. One of the most challenging and attractive topics in this field is the preparation of high oxidation states of Hg.[1, 2] Group IIB elements, including Zn, Cd, and Hg are usually defined as post-transition metals[3] because they are commonly oxidized only to the +2 state.[4, 5] Their *d* shells are completely filled and do not participate in the formation of chemical bonds; however, there is a high expectation that Hg should be stable at higher oxidation states due to the large relativistic effects that increase the energies of its *5d* levels.

Earlier attempts focused on HgF<sub>4</sub> molecules in gas phases, including several quantum chemistry calculations on the molecule.[6–13] It was predicted that HgF<sub>4</sub> molecules can resist dissociation to HgF<sub>2</sub> and F<sub>2</sub> molecules. [9, 14, 15] However, the thermodynamically stable form of HgF<sub>2</sub> at low temperatures is the solid phase rather than the gas phase.[2] HgF<sub>4</sub> molecules in the gas phase or in molecular crystals can, therefore, become unstable and dissociate to form HgF<sub>2</sub> and F<sub>2</sub>, as predicted by our calculations (see below). For this reason, the synthesis of HgF<sub>4</sub> molecules has shown to be extremely difficult. Recently, after numerous experimental attempts, the trace of HgF<sub>4</sub> molecules was observed using matrix-isolation infrared (IR) spectroscopy.[1] The HgF<sub>4</sub> molecules were unstable and dissociated to yield HgF<sub>2</sub> and F<sub>2</sub> within very short periods of time. To demonstrate that Hg is truly a transition metal, one must *thermodynamically* stabilize a Hg center in the +4 oxidation state.

In this letter, we propose a totally new approach that utilizes high-pressure techniques to stabilize Hg<sup>4+</sup> in the solid phase. Over the past several decades, high-pressure methods based on diamond anvil cells (DACs)

have yielded novel structures of elements and compounds under extremely high pressures (beyond megabars). This field has been particularly advanced by the recent development of first-principles structure-searching methods that can predict high-pressure structures to extremely high accuracy without experimental or intuited input. For example, the recently implemented particle swarm optimization (PSO) technique [16, 17] successfully predicted the high-pressure structures of various systems, including lithium[18], water ice[19], and Bi<sub>2</sub>Te<sub>3</sub>. [20] In most high-pressure studies, the oxidation states of the compounds remain the same at high pressures. We show here that the high-pressure techniques have the potential to provide a controllable method for achieving unusual oxidation states.

We conducted a structure search over the full structure configuration space, based on *ab initio* total-energy calculations and a PSO technique, implemented in the CALYPSO (crystal structure analysis by particle swarm optimization) code.[16, 17] The underlying *ab initio* structural relaxations and electronic band structure calculations were performed using the framework of density functional theory (DFT), implemented in the VASP code.[21] The generalized gradient approximation (GGA) in the framework of Perdew–Burke–Ernzerhof (PBE)[22] was used to treat the exchange-correlation functional, and the projector augmented wave (PAW)[23] pseudopotentials were used to describe the ionic potentials. The cutoff energy for the expansion of the wave function into plane waves was set to 700 eV, and the Monkhorst–Pack *k* meshes [24] were chosen to ensure that all enthalpy calculations converged to better than 1 meV/atom. The structure searches were performed with a unit cell containing 20 atoms (4 Hg and 16 F) and were performed over the pressure range 0–300 GPa. The phonon spectra

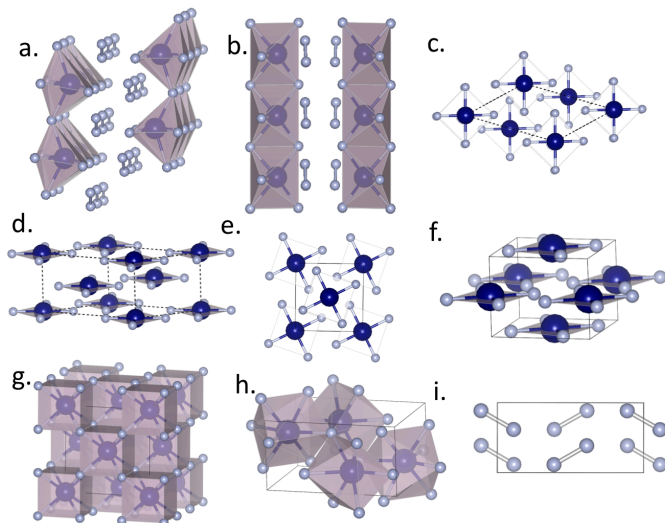


FIG. 1: (Color figures available online.) (a) and (b): Two views of the  $Pca2_1$  structure, the optimized lattice parameters at 15 GPa are  $a = 14.183$  ,  $b = 3.478$  and  $c = 4.153$  with Hg occupying 4a (0.082, 0.277, 0.486) and F occupying 4a (0.309, 0.530, 0.321), 4a (0.306, 0.173, 0.523), 4a (0.663, 0.211, 0.337) and 4a (0.521, 0.771, 0.982) positions; (c) side view and (d) top view of the  $I4/m$  structure, the optimized lattice parameters at 150 GPa are  $a = 4.366$  and  $c = 3.498$  with Hg occupying 2b (0, 0, 0.500) and F occupying 8h (0.304, 0.888, 0) positions; (e) top view and (f) side view of the  $I4/mmm$  structure; (g) the  $CaF_2$  structure; (h) the  $HgCl_2$  structure; (i) the  $F_2$  molecular crystal structure. The large dark-blue balls and the small light-grey balls indicate Hg and F atoms, respectively. Parameters of more related structures can be found in the online supplementary materials.

were calculated using the Phonopy program.[31]

As shown in Fig. 2(a), two thermodynamically stable structures were identified over the pressure range of 0–300 GPa. The most stable structure under ambient conditions had a symmetry of  $Pca2_1$  and consisted of chain-like  $HgF_2$  and  $F_2$  molecules [Fig.1(a) and (b)], indicating that at low pressures, the  $Hg_1-F_4$  system tended to decompose into  $HgF_2$  and  $F_2$ . The shortest F-F distances were  $1.485 \text{ \AA}$  at 0 GPa, similar to the F-F bond length in the gas phase.[25] At a pressure of 20 GPa, the system transformed into a structure with  $I4/m$  symmetry [Fig.1(c) and (d)]. This structure consisted of  $HgF_4$  molecules and each Hg had four nearest neighboring F atoms. At 50 GPa, the Hg-F distance was  $1.949 \text{ \AA}$ . This distance was significantly shorter than the average Hg-F distance of  $2.215 \text{ \AA}$  at the same pressure. On the other hand, the shortest F-F distance was  $2.112 \text{ \AA}$  which was significantly longer than the F-F molecular bond length of  $1.439 \text{ \AA}$ , indicating that the molecular features of  $F_2$  were destroyed upon formation of the  $HgF_4$  molecules. The structural parameters for both structures and the dependence of bond lengths in  $I4/m$  structure on increasing pressure can be found in the online supplemental material.

Another structure displayed a symmetry of  $I4/mmm$

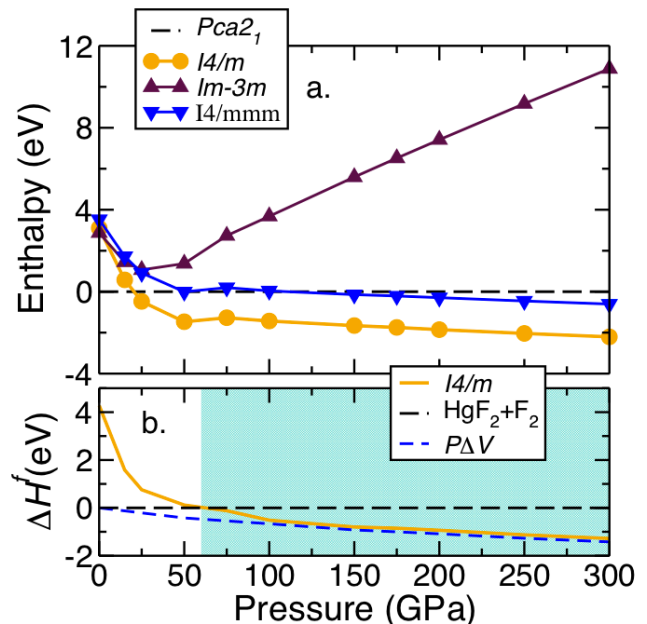


FIG. 2: (Color figures available online.) (a) Comparison of the enthalpies as a function of the pressure for the  $Hg_1-F_4$  structures selected from the PSO search. The results are reported with respect to the enthalpy of the  $Pca2_1$  structure, which is the most stable structure under ambient conditions. (b) Energy of the  $HgF_2(s) + F_2(s) \rightarrow HgF_4(s)$  reaction. The enthalpy of  $HgF_4$  was obtained from the  $I4/m$  structure. The blue dashed line shows the enthalpy gain due to the volume reduction,  $P\Delta V$ . The area shaded in light blue indicates the range of pressures under which  $HgF_4$  is thermodynamically stable at 0 K.

[Fig. 1(e) and 1(f)]. Although this structure appeared similar to the  $I4/m$  structure as viewed from the top, each Hg atom was bonded to eight F atoms to form a chain. The enthalpy of this structure was lower than that of the  $Pca2_1$  structure at 100 GPa; however, over the pressure range 0–300 GPa, the enthalpy exceeded that of the  $I4/m$  structure, a  $HgF_4$  molecular crystal.

As shown experimentally[26, 27] and in our calculations,  $HgF_2$  was stable in extended solid structures other than the  $HgF_2$  chains present in the  $Pca2_1$  structure of the  $Hg_1-F_4$  system. To determine whether the separated  $HgF_2$  and  $F_2$  phases could react to form a  $HgF_4$  phase, we calculated the energy of the  $HgF_2(s) + F_2(s) \rightarrow HgF_4(s)$  reaction. The structures of  $HgF_2$  and  $F_2$  under pressure were searched using the PSO method.  $HgF_2$  was found to be stable in the  $CaF_2$  structure at 0 to 100 GPa,[26, 27] in the low-pressure structure of  $HgCl_2$  ( $Pnma$ )[28] from 100 to 300 GPa. We also found that  $F_2$  maintained its molecular features and was stable in its low-pressure structure  $C12/c1$ [29] up to 300 GPa.

As shown in Fig. 2(b), our results clearly showed that at ambient pressures, the separated  $HgF_2$  and  $F_2$  phases were stable against the formation of  $HgF_4$ , *i.e.* the reaction energy was positive. The reaction energy decreased rapidly as the pressure increased and becomes negative

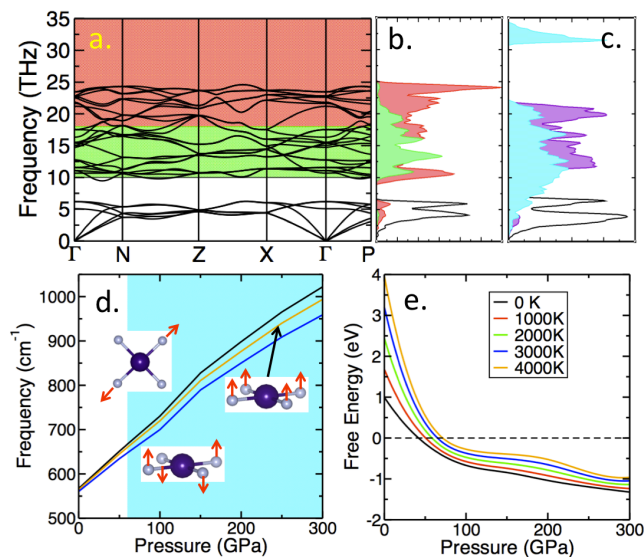


FIG. 3: (Color figures available online.) (a) Phonon spectrum of the  $\text{HgF}_4$  molecular crystal in the  $I4/m$  structure under a pressure of 150 GPa. The energy regions that corresponded to the F in-plane, the F out-of-plane, and the Hg motions are shaded in red, green, and white. (b) The phonon projected density of states (PDOS) of  $\text{HgF}_4$  in the  $I4/m$  structure at a pressure of 150 GPa. The black line and the red and green shaded areas show the DOS projected onto the Hg, the F in-plane, and the F out-of-plane motions. (c) The summed phonon PDOS of  $\text{HgF}_2$  in the  $Pnma$  structure and  $\text{F}_2$  in the  $C12/c1$  structure at 150 GPa. The black line shows the motions of Hg in  $\text{HgF}_2$ . The blue and purple shaded areas show the motions of F in the  $\text{HgF}_2$  and  $\text{F}_2$  solids, respectively. (d) The three selected  $I4/m$  phonon frequencies at  $\Gamma$  as a function of the pressure. The black, orange, and blue lines denote the Hg-F stretching and bending modes, as shown in the insets. (e) The calculated reaction free-energies as a function of the pressure at 0, 1000, 2000, 3000, and 4000 Kelvin.

at 60 GPa, indicating that  $\text{HgF}_4$  became thermodynamically stable. The energy gain upon formation of the  $\text{HgF}_4$  molecules was quite large and increased significantly with the increasing pressure. At a pressure of 150 GPa, the energy gain was 0.8 eV or 77 kJ/mole, providing a large driving force for oxidation of Hg to the +4 state.

The phonon spectrum of  $\text{HgF}_4$  in the  $I4/m$  structure, of  $\text{HgF}_2$  in the  $Pnma$  structure, and of  $\text{F}_2$  in the  $C12/c1$  structure were calculated over the pressure range of 0–300 GPa. The results show that the structures of all three solids were dynamically stable up to 300 GPa, *i.e.* none of the phonon modes featured imaginary frequencies. As shown in Fig. 3(a) and (b), the low-frequency modes of the  $\text{HgF}_4$  molecular crystal at 150 GPa (from 0 to 10 THz) were dominated by the motions of the Hg atoms, whereas the modes in the frequency range 10–18 THz and 18–25 THz were dominated by the F out-of-plane ( $z$ ) and in-plane ( $x$  and  $y$ ) motions. The Hg-F stretching modes in  $\text{HgF}_4$  reached their peaks at 24 THz ( $800 \text{ cm}^{-1}$ ). On the other hand, the Hg-F stretching modes in  $\text{HgF}_2$  reached their peak around 20 THz ( $650 \text{ cm}^{-1}$ ), as shown in Fig. 3(c). The F-F stretching modes were much

higher in energy, and a frequency gap was observed from 21 to 31 THz ( $700\text{--}1000 \text{ cm}^{-1}$ ) in a  $\text{HgF}_2$  and  $\text{F}_2$  mixed sample. The vibrational peak observed in this gap will indicate the formation of  $\text{HgF}_4$  molecular crystals. The  $\text{HgF}_4$  vibrational modes in this frequency gap included Hg-F stretching and bending modes and could be either IR or Raman active. As shown in Fig. 3(d), the frequencies of these peaks tended to split under higher pressures, indicating a broadening of the  $\text{HgF}_4$  signature peaks with increasing pressure.

Another important issue associated with the synthesis of  $\text{HgF}_4$  in a high-pressure DAC is the persistence of the stable structure at high temperatures. Although  $\text{HgF}_4$  is thermodynamically stable at 0 K, it does not form easily at very low temperatures in a DAC because of the large kinetic barrier to the solid-state reaction. To overcome this barrier, thermo-heating or laser-heating techniques may be used to increase the temperature in the DAC up to a few thousand degrees Kelvin. We calculated the reaction energies at finite temperatures using the calculated phonon spectra of the  $\text{HgF}_4$ ,  $\text{HgF}_2$ , and  $\text{F}_2$  solids. As shown in Fig. 3(e), elevated temperatures tended to destabilize the  $\text{HgF}_4$  solid; however, even at  $T = 4000 \text{ K}$ ,  $\text{HgF}_4$  could still reach thermodynamic stability at pressures exceeding 75 GPa.

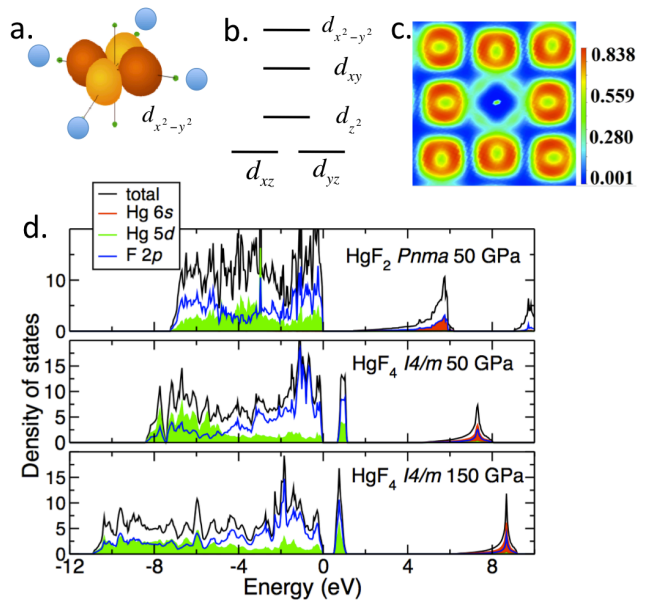


FIG. 4: (Color figures available online.) (a) The crystal field splitting diagram of a square planar complex; the light-blue balls indicate the F anions and the orange and red spheres indicate the  $d_{x^2-y^2}$  orbit; (b) the  $d$  orbitals were split under the square planar crystal field; (c) the calculated electron localization function (ELF) for  $\text{HgF}_4$  in the  $I4/m$  structure at 150 GPa; (d) the calculated PDOS for  $\text{HgF}_2$  in the  $\text{HgCl}_2$  structure at 50 GPa and for the  $\text{HgF}_4$  molecular crystal in the  $I4/m$  structure at 50 and 150 GPa. In the PDOS plots, the black solid lines indicate the total DOS, the blue solid lines indicate the F  $2p$  states, the red and green shaded areas indicate the Hg  $6s$  and  $5d$  states.

The planar geometry of the  $\text{HgF}_4$  molecules is typical of  $d^8$  configurations, indicating the involvement of  $5d$  electrons in the formation of Hg-F bonds. As shown in Fig. 4(a) and (b), the  $d$  orbitals split into four groups in a square planar crystal field due to differences in the interactions with the four surrounding F anions. Among these orbitals,  $d_{x^2-y^2}$  was the highest in energy. The transition metal cations could be energetically stabilized in this configuration in the event that 8 electrons filled the 4 lower  $d$  states and left the  $d_{x^2-y^2}$  states empty. The bonding features of  $\text{HgF}_4$  were also examined by calculating the electron localization function (ELF)[32] using the VASP code. The results [Fig. 4(c)] clearly showed the equivalent covalent bonds of Hg and its four neighboring F atoms.

More direct evidence for the involvement of  $d$  electrons in the formation of chemical bonds with F was obtained from the projected density of states (PDOS). We calculated and compared the total DOS and PDOS for  $\text{HgF}_4$  in the  $I4/m$  structure and  $\text{HgF}_2$  in the  $\text{HgCl}_2$  structure at 50 GPa.  $\text{HgF}_2$  revealed a gap of 1.5 eV. The conduction bands consisted mainly of the F  $p$  and Hg  $6s$  states, whereas the valence bands consisted of both F  $p$  and Hg  $5d$  states [Fig. 4(d)]. The PDOS showed that all  $5d$  states were filled, and Hg was apparently in the +2 state. On the other hand,  $\text{HgF}_4$  displayed a much smaller gap of only 0.71 eV. More importantly, the  $5d$  states were distributed over both the valence and the conduction bands, indicating that the  $5d$  electrons were depleted, in agreement with the planar geometry of the  $\text{HgF}_4$  molecules and the  $d^8$  configuration analysis.

Several effects of the high pressure assist in stabilizing the  $\text{HgF}_4$  molecules. One mechanism is based on the crystal field splitting. Because high pressures reduce the inter-atomic distances, including those between Hg and its neighboring F atoms, the high pressures enhance the crystal field splitting. As a result, the energy of the  $d_{x^2-y^2}$  state increases with increasing pressure. The PDOS of  $\text{HgF}_4$  in the  $I4/m$  structure at 150 GPa is shown in Fig. 4(d). A comparison with the PDOS at 50 GPa shows that although the gap changed only slightly with increasing pressure, the center of the F  $2p$  states was significantly lower relative to the  $d_{x^2-y^2}$  state, indicating a larger energy gain with electron transfer from the  $5d$  to the  $2p$  orbital at higher pressures. Another important factor is the reduction of the volume during the formation of solid  $\text{HgF}_4$ . This factor further increases the enthalpy gain. As shown in Fig. 2(b), the value of  $P\Delta V$  increased with increasing pressure. Although its contribution to the enthalpy gain was small at low pressures, this contribution became dominant at pressures exceeding 50 GPa. The reduction in the volume arose from the shortening of Hg-F bonds as Hg changed from the +2 to the +4 oxidation states due to the involvement of the  $5d$  electrons in the formation of stronger Hg-F bonds with a

larger covalent component. When the enthalpy gain was sufficiently large, the reaction  $\text{HgF}_2(\text{s})+\text{F}_2(\text{s}) \rightarrow \text{HgF}_4(\text{s})$  became exothermic and  $\text{HgF}_4$  became thermodynamically stable. As calculated, this occurred at 60 GPa.

In summary, we demonstrated that under an external pressure applied using the DAC technique, Hg could be thermodynamically stabilized in a high oxidation state to form solid structures of  $\text{HgF}_4$  molecules. The atomic structure and the electronic structure of the high-pressure phases suggested that the  $5d$  orbitals of Hg were involved in chemical bonding. Thus, our calculations suggested that Hg behaves as a true transition metal under high pressures. High-pressure techniques have been used to alter the chemical inertness of noble gases and to sustain them in unusual chemical states.[33–35] Our study also suggests that high-pressure techniques may be used as a controllable method to achieve unusual oxidation states in matter.

**Acknowledgement** MSM thanks Prof. Ram Seshadri for inspiring discussions on the high oxidation states of transition metals. MSM also thanks the ConvEne-IGERT Program (NSF-DGE 0801627). XW was partially supported by the National Natural Science Foundation of China (Grant N 11147007). YM was supported by the National Natural Science Foundation of China (Nos. 11025418 and 91022029)

---

\* Electronic address: miaoms@mrl.ucsb.edu

- [1] X. Wang, L. Andrews, S. Riedel, M. Kaupp, *Angew. Chem.* **119**, 8523 (2007).
- [2] W. B. Jensen, *J. Chem. Edu.* **85**, 1182 (2008).
- [3] A. D. McNaught and A. Wilkinson, *IUPAC Compendium of Chemical terminology*, 2nd ed. Blackwell Sci. 1997.
- [4] N. N. Greenwood and A. Earnshaw, *Chemistry of the Elements*, Pergamon, Oxford, 1984.
- [5] F. A. Cotton, G. Wilkinson, C. A. Murillo, and M. Bockman, *Advanced Inorganic Chemistry*, 6th ed., Wiley, New York, 1999.
- [6] R. L. Deming, A. L. Allred, A. R. Dahl, A.W. Herlinger, M. O. Kestner, *J. Am. Chem. Soc.*, **98**, 4132 (1976).
- [7] C. K. Jørgensen, *J. Chim. Phys.* **76**, 630 (1979).
- [8] C. K. Jørgensen, *Z. Anorg. Allg. Chem.*, **91**,540 (1986).
- [9] S. Riedel, M. Straka, M. Kaupp, *Phys. Chem. Chem. Phys.*, **6**, 1122 (2004).
- [10] W. Liu, R. Franke, M. Dolg, *Chem. Phys. Lett.*, **302**, 231 (1999).
- [11] P. Pyykkö, M. Straka, M. Patzschke, *Chem. Commun.*, 1728 (2002).
- [12] P. Hrobarik, M. Kaupp, S. Riedel, *Angew. Chem.* **120**, 8759 (2008).
- [13] S. Riedel, M. Straka, M. Kaupp, *Chem. Eur. J.* **11**, 2743 (2005).
- [14] M. Kaupp and H. G. von Schnering, *Angew. Chem.* **105** 952 (1993); *Angew. Chem. Int. Ed. Engl.* **32**, 861 (1993).
- [15] M. Kaupp, M. Dolg, H. Stoll and H. G. von Schnering, *Inorg. Chem.* **33**, 2122 (1994).
- [16] Y. Wang, J. Lv, L. Zhu and Y. Ma, *Phys. Rev. B* **87**, 094116 (2010).
- [17] Y. Ma, Y. Wang, J. Lv, and L. Zhu,

lab.jlu.edu.cn/~calypso.html.

- [18] J. Lv, Y. Wang, L. Zhu, and Y. Ma Phys. Rev. Lett. **106**, 015503 (2011).
- [19] Y. Wang, H. Y. Liu, J. Lv, L. Zhu, H. Wang and Y. Ma, Nature Commun. **2**, 563 (2011).
- [20] L. Zhu, H. Wang, Y. Wang, J. Lv, Y. Ma, Q. Cui, Y. Ma and G. Zhou, Phys. Rev. Lett. **106**, 145501 (2011).
- [21] G. Kresse and J. Fürthmüller, Phys. Rev. B **54**, 11169 (1996).
- [22] J. P. Perdew, K. Burke, and M. Ernzerhof, Phys. Rev. Lett. **77**, 3865 (1996).
- [23] P. E. Blöchl, Phys. Rev. B **50**, 17953 (1994).
- [24] H. J. Monkhorst and J. D. Pack, Phys. Rev. B **13**, 5188 (1976).
- [25] M. W. Chase, C. A. Davies, J.R. Downey, D. J. Frunip, R. A. McDonald and A. N. Syverud, J. Phys. Chem. Ref. Data Suppl., **14**, 695 (1985).
- [26] R. T. Poole, J. A. Nicholson, J. Liesegang, J. G. Jenkin, and R. C. G. Leckey, Phys. Rev. B **20**, 1733 (1979).
- [27] M. Hostettler and D. Schwarzenbach, C. R. Chimie, **8**, 147 (2005).
- [28] Subramanian, V. Seff, K. Acta Crystallographica B **36**,2132 (1980).
- [29] L. Pauling, I. Keaveny and A. B. Robinson, J. Solid State Chem. **2**, 225 (1970).
- [30] W. Cochran, Phys. Rev. Lett. **3**, 412 (1959).
- [31] Program Phonopy available at <http://phonopy.sourceforge.net/>, the force constants matrix is determined by VASP. Convergence test gave the use of a 2 x 2 x 2 supercell.
- [32] A. D. Becke, K. E. Edgecombe, J. Chem. Phys. **92**, 5397 (1990).
- [33] A. P. Japhcoat, Nature **393**, 355 (1998).
- [34] M. Somayazulu, P. Dera, A. F. Goncharov, S. A. Gramsch, P. Liermann, W. Yang, Z. Liu, H. K. Mao, R. J. Hemley, Nature Chem. **2**, 50 (2010).
- [35] W. A. Caldwell, J. H. Nguyen, B. G. Frommer, F. Mauri, S. G. Louie, R. Jeanloz, Science **277**, 930 (1997).